

# Expand Dimensional of Seismic Data and Random Noise Attenuation Using Low-Rank Estimation

Javad Mafakheri , Amin Roshandel Kahoo , Rasoul Anvari ,  
Mokhtar Mohammadi, Mohammad Radad , and Mehrdad Soleimani Monfared 

**Abstract**—Random noise attenuation in seismic data requires employing leading-edge methods to attain reliable denoised data. Efficient noise removal, effective signal preservation and recovery, reasonable processing time with a minimum signal distortion and seismic event deterioration are properties of a desired noise suppression algorithm. There are various noise attenuation methods available that more or less have these properties. We aim to obtain more effective denoised seismic data by assuming 3-D seismic data as a tensor in order three and increasing its dimension to 4-D seismic data by employing continuous wavelet transform (CWT). First, we map 3-D block seismic data to smaller blocks to estimate the low-rank component. The CWT of the tensor is calculated along the third dimension to extract the singular values and their related left/right vectors in the wavelet domain. Afterward, the effective low-rank component is extracted using optimized coefficients for each singular value. Thresholding is applied in the wavelet domain along the third dimension to calculate effective coefficients. Two synthetic and field data examples are considered for performance evaluation of the proposed method, and the results were compared with the competitive random noise suppression methods, such as the tensor optimum shrinkage singular value decomposition, the iterative block tensor singular value thresholding, and the block matching 4-D algorithms. Qualitative and quantitative comparison of the proposed method with other methods indicates that the proposed method efficiently eliminates random noise from seismic data.

**Index Terms**—Continuous wavelet transform (CWT), low-rank matrix, optimal shrinkage, singular value decomposition, seismic random noise.

## I. INTRODUCTION

**R**ANDOM noise attenuation of acquired seismic data is continuously under research to attain techniques with higher efficiency. Besides difficulties in designing efficient filters, the nature of random noise in seismic data widely differs

Manuscript received July 28, 2021; revised March 1, 2022; accepted March 23, 2022. Date of publication March 28, 2022; date of current version April 18, 2022. (Corresponding author: Rasoul Anvari.)

Javad Mafakheri, Amin Roshandel Kahoo, Rasoul Anvari, and Mohammad Radad are with the School of Mining, Petroleum and Geophysics Engineering, Shahrood University of Technology, Shahrood 4851878195, Iran (e-mail: javadmafakheri6104@gmail.com; roshandel@shahroodut.ac.ir; rasoulanvaris93@gmail.com; mradad@shahroodut.ac.ir).

Mokhtar Mohammadi is with the Department of Information Technology, College of Engineering and Computer Science, Lebanese French University, Kurdistan Region 44001, Iraq (e-mail: mokhtar.mohammadi1@gamil.com).

Mehrdad Soleimani Monfared is with the School of Mining, Petroleum and Geophysics Engineering, Shahrood University of Technology, Shahrood 4851878195, Iran, and also with the Karlsruhe Institute of Technology (KIT), Geophysical Institute, 76131 Karlsruhe, Germany (e-mail: msoleimani@shahroodut.ac.ir, mehrdad.soleimani@partner.kit.edu).

Digital Object Identifier 10.1109/JSTARS.2022.3162763

in source and characteristics, which require complex diffusion filter design for efficient noise attenuation methods [1]. Characteristics of seismic random noise have been thoroughly reviewed in various studies [2]. These characteristics are statistical parameters, geological environment that the seismic data were acquired on and other parameters that depict the nature of seismic noise [3]. Several studies stated that the seismic random noise in different environments, such as desert, hilly, and grassland areas, exhibits diverse characteristics [4]–[6]. For instance, the more geological complex media, the less linearity behavior in the random noise. In addition, as the nature of seismic random noise, they are generally considered as stationary series in short length windows, which imposes application of adaptive and amplitude preserving methods [7]. By revealing the importance of signal preservation by filtering seismic data, conventional noise removal techniques are known to be less effective and impressive for complete preservation and/or recovery of the seismic signal. Hence, diverse methods utilizing miscellaneous concepts were introduced. Some techniques consider the random noise attenuation as a model selection procedure employing the elimination among a set of various models [8]. This group of methods benefits from automatic threshold definition, but they require making the best approximate model, resembling properties of noise [9]. It was disclosed that this procedure performs effectively on seismic data contaminated by random noise in minor to moderate levels. Still, it loses out in handling highly contaminated seismic data [10]. Nevertheless, this problem was resolved by implementing the wave-separation technique. Using this technique entails acquiring seismic data in three components, which is rather impressive but infeasible in common reflection seismic acquisition practice [11]. Another impressive method is the anisotropic nonlinear diffusion filter, which enhances seismic signal while preserving details of seismic events and controls resolution. Notwithstanding, its performance dwindles in dealing with seismic data acquired from subsurface complex geological structure [12]. This obstacle was later partially resolved by the introduction of low-rank estimation methods, block matching 3-D and block matching 4-D (BM4D) methods, iterative block tensor singular value thresholding (IBTSVT), adaptive fission particle filtering, time-frequency peak filtering (TFPF), hyperbolic trace-, amplitude preserving-, adaptive window length-, multiple directional-, and optimal spatiotemporal TFPF methods [13]–[15]. Other recently introduced techniques, such as smooth patch ordering-based nonlocal means, fractal conservation law, and bidimensional EMD are still under investigation for proper noise removal in seismic data [16]–[18]. Among these numerous noise suppression methods, BM4D and IBTSVT methods found wide practical applications in seismic random noise attenuation [19], [20]. It was also shown that

the combination of the sparse decomposition and the low-rank matrix could effectively be used in heavy noise-contaminated data [21]. The low-rank estimation methods prerequisites the Hankel matrix to be low-rank in the  $f - x$  domain. To achieve this goal, the optimal shrinkage of singular values known as the tensor optimum shrinkage singular value decomposition (t-OSSVD) method was recently introduced [22]. The t-OSSVD method optimally recovers the low-rank matrices from noisy data and sufficiently suppresses random noise. The sparsity in the t-OSSVD could be used to provide an appropriate balance in essential characteristics of any desired filtering, the noise removal, and feature preservation [23]. Therefore, we will introduce a novel strategy to obtain the more effective denoised seismic data. We divide 3-D seismic data into smaller blocks and also improve its performance in random noise attenuation by employing the concept of continuous wavelet transform (CWT) through the extraction of singular values using the optimum shrinkage technique in a new 4-D seismic data (X, Y, t, F) in which X, Y, t, and F imply the X-line, in-line, time samples, and frequency dimensions. The capabilities of the proposed method then would be evaluated through the application on synthetic and real field seismic data examples. The results will be compared with the results of the t-OSSVD, IBTSVT, and the BM4D methods. Qualitative and quantitative comparison between results will demonstrate the capabilities of the proposed method against other competitive techniques and worthwhile improvement to the t-OSSVD method.

## II. PROPOSED METHOD

Noise-free seismic data exhibit low-rank characteristic, which is an ideal property both in the original and transformed domains of data for ideal application of further signal analysis [24]. Two major categories of methods for random noise removal are matrix rank reduction and low-rank and sparse components decomposition. The proposed strategy here is based on the latter category of noise suppression methods. In this article, we decompose the 3-D seismic data into a concatenation of blocks of the same size, then we extract low-rank component of each block by minimizing the tubal rank of each block tensor by optimal reweighting of the singular vectors of the measurement matrix.

### A. Tensor Singular Value Decomposition (t-SVD)

Considering the last developed and efficient RPCA, the seismic data matrix when defined by  $\chi \in \mathbb{R}^{n_1 \times n_2}$  and it has geometric repetitive structures, it would be decomposed to sparse component,  $S$ , and a low-rank component  $L$  which defines [25]

$$\chi = L + S. \quad (1)$$

Through modeling this equation as a convex optimization problem it reads

$$\min_{L,S} \|L\|_* + \lambda \|S\|_{1,1,2} \quad (2)$$

where the nuclear norm is defined by  $\|L\|_*$ , the  $\|S\|_{1,1,2}$ , is defined as  $\sum_{i,j} \|S(i, j, :)\|_F$ , and the parameter  $\lambda$  is calculated by  $\lambda = 1/\sqrt{\max(n_1, n_2)}$ .

Considering the 3-D matrix of seismic data, it is problematic to define a fixed definition for its rank number, however, through dividing the 3-D seismic data into equal size blocks, the low-rank

component of each block could be defined by employing the rank-based theory [26]. Through this definition,  $L_p$  and  $S_p$  are low-rank component and sparse component of a 3-D seismic data,  $\chi \in \mathbb{R}^{n_1 \times n_2 \times n_3}$ , respectively. The tensor robust principal component uses the t-SVD method, which reads

$$\chi = u * s * \nu^T \quad (3)$$

where  $u$  illustrates the orthogonal 3-D matrix of size  $n_1 \times n_1 \times n_3$  and  $\nu$  depicts also the orthogonal 3-D matrix but with the  $n_2 \times n_2 \times n_3$ . The parameter  $s$  is a  $f$ -diagonal 3-D matrix with the same size of  $\chi$ . Through concatenating the low-rank components for the entire 3-D small blocks, the principal components of the multiway data would be defined [27]. Based on this methodology, we propose a novel sparse and low-rank extraction method in the CWT domain.

### B. Sparse and Low-Rank Component Extraction

The most efficient and distinguishable representation in transformed domain commonly is obtained via sparse transform [28]. Therefore, the sparse transform-based random noise attenuation methods are widely used in the literature of the seismic data processing methods [29]–[32]. Hence, the proposed methodology is based on the optimal weighting coefficients of wavelet transform by squeezing normal vectors and singular values of the wavelet transform. By considering the CWT of the signal  $x(t)$  as [33]

$$W_x(a, b) = \frac{1}{\sqrt{a}} \int x(t) \Psi^* \left( \frac{t-b}{a} \right) dt. \quad (4)$$

The complex conjugate of the mother wavelet is defined by  $\Psi^*$  and the parameters  $a$  and  $b$  represent the scale parameter and the time shift of the mother wavelet, respectively. Bandpass filters that are oscillatory in the time domain are mother wavelet functions of interest. As a result, for large values of  $a$ , the basis function becomes a stretched version of the mother wavelet, i.e., a contracted version of the mother wavelet, which is a short-duration, high-frequency function, is used as the basis function for minor values of  $a$ . The wavelet's translation is defined by parameter  $b$ , which allows for time localization.  $\Psi(t)$  is a bandpass signal that should decay quickly enough to provide enough time resolution. For the development of the CWT, the Morlet wavelet is a suitable example of a mother function. It is characterized by [34], [35]

$$\Psi(t) = \left[ e^{-i2\pi f_0 t} - e^{-2\pi^2 f_0^2 \sigma^2} \right] e^{-\frac{t^2}{2\sigma^2}} \quad (5)$$

where  $\sigma$  is the duration of this wavelet signal. Another example of mother wavelet is the Ricker wavelet that it is defined as [36]

$$\Psi(t) = \left( 1 - \frac{1}{2} \omega_p^2 t^2 \right) \cdot e^{(-\frac{1}{2} \omega_p^2 t^2)}. \quad (6)$$

If the most energetic frequency is  $\omega_p$  (in radians per second), it has a zero mean and is symmetric in the time domain.

The CWT of the seismic signal  $x(t)$  would be obtained through correlation of the seismic signal with various scaled and translated forms of the mother wavelet [37]. By definition, the SVD of the matrix  $W_x(a, b)$  is known as the  $U\Sigma V^H$ , where  $U$  and  $V$  depict the right and the left vectors and the diagonal matrix of singular values of CWT is defined by  $\Sigma$ . In the t-SVD method, some of the data singular values shrink to zero, while the others remain unchanged [38]. By considering

the condition of  $\eta : [0, \infty) \rightarrow [0, \infty)$ , there would be a singular value shrinkage estimator for a matrix with the size of  $m \times n$  for any specific choice of scalar values, which is defined by the following equation, known as the shrinking operator

$$\hat{X}_\eta = \sum_{i=1}^m \eta(y_i) \nu_i \tilde{v}_i' \quad (7)$$

where  $y_i$ ,  $\nu_i$ , and  $\tilde{v}_i'$  are singular values, the left vector, and transpose of the right vector, respectively. By considering the general definition of a seismic signal, which is sum of noise free data  $S$  and random noise  $W$  as  $\chi = S + W$ , the signal is defined as

$$S = \sum_{i=1}^r \theta_i u_i \hat{u}_i' \quad (8)$$

where the effective-rank noise free data are depicted by  $r$  and  $\theta_i$  represents the singular value. The denoising problem in the proposed method is formulated as a weighted approximation problem as

$$w_{\text{opt}} := \underset{\|w\|_{\ell_0} = r}{\text{arg min}} \left\| \sum_{i=1}^r \theta_i u_i \hat{u}_i' - \sum_i w_i \nu_i \tilde{v}_i' \right\|_F. \quad (9)$$

The  $w_i^{\text{opt}}$  represents the thresholding and shrinkage operator on the singular values of  $\chi$ . It should be noted that the optimization problem in (7) seems to be unobservable since it depends on an unknown matrix desired to be estimated; however, the optimal solution itself is computable. No structure was assumed to find the optimal solution except the low-rank characteristic in the signal matrix. However, it is known that the exploitable structure is present in the noise portion of the eigen-spectrum, i.e., the  $\min(m, n) - r$  singular values of  $\chi$ . The advantage of the proposed algorithm over the optimization problem in (7) is that the presented algorithm uses an estimate of the rank of the signal matrix as input data and will return the (re)weighted approximation, which efficiently mitigates the effect of rank overestimation. When  $\sigma_1 > \sigma_2 > \dots > \sigma_n$  represents the order of the singular values of observed data, and  $w \in \mathbb{R}^l$  the squared error of the presented procedure would be defined by

$$SE(w) = \|S - \sum_{i=1}^l w_i \nu_i \nu_i^H\|_F^2. \quad (10)$$

Consider the denoising optimization problem

$$w_{\text{opt}} := \underset{w = [w_1, w_2, \dots, w_r]^T \in \mathbb{R}_+^r}{\text{arg min}} SE(w). \quad (11)$$

An efficient approximate solution to (9) was presented as [39]

$$\hat{w}_{i, \hat{r}}^{\text{opt}} = -2 \frac{\hat{D}(\hat{\sigma}_i; \hat{\Sigma}_{\hat{r}})}{\hat{D}'(\hat{\sigma}_i; \hat{\Sigma}_{\hat{r}})} \quad (12)$$

where  $\hat{\sigma}_i$  is the  $i$ th large singular value corresponding to the order of the effective rank and  $\hat{\Sigma}_{\hat{r}} = \text{diag}(\hat{\sigma}_{r+1}, \dots, \hat{\sigma}_q) \in \mathbb{R}^{(n-\hat{r}) \times (m-\hat{r})}$ . It was supposed that the observed data have  $q$  singular values.  $\hat{D}(\hat{\sigma}_i; \hat{\Sigma}_{\hat{r}})$  defines the D-transform and the derivative of the D-transform is defined by  $\hat{D}'(\hat{\sigma}_i; \hat{\Sigma}_{\hat{r}})$ .

---

### Algorithm 1: Proposed Method for Denoising 3-D Seismic Data.

---

**Input: 3-D seismic data-plus-noise**  $\chi \in \mathbb{R}^{n_1 \times n_2 \times n_3}$ ,  
 B=Block size, proper wavelet parameters, r = Estimate of the effective rank of the low-rank signal matrix  
 $L = X \in \mathbb{R}^{n_1 \times n_2 \times n_3} = 0$   
 Divide 3-D data to 3-D small blocks  
 For each block  
 For i = 1 to length (X-line)  
 For j = 1 to length (in-line) do  
 Convert to 4D  $\leftarrow CWT(B, [], 3)$   
 Compute:  
 $\chi = u * s * \nu^T$   
 $\hat{\sigma}_{\hat{r}} = \text{diag}(\hat{\sigma}_{r+1}, \dots, \hat{\sigma}_q) \in \mathbb{R}^{(n-\hat{r}) \times (m-\hat{r})}$   
 Estimate  $\hat{w}_{t, \hat{r}}^{\text{opt}}$  using (10)  
 Recover denoised section as  $S = \sum_{i=1}^r \hat{w}_{t, \hat{r}}^{\text{opt}} u_i \hat{u}_i'$   
 Apply inverse wavelet transform on  $S$   
 Replace  $S$  in  $L$  as denoised 3D seismic data  
 End for  
 End for  
 End for  
 concatenation effective parts

---

### C. Proposed Algorithm

Based on the abovementioned motivation, we decompose the 3-D seismic data into a concatenation of blocks of the same size, then CWT is applied on the third dimensional and provides a 4-D tensor. The low-rank component of each block is extracted by minimizing the tubal rank of each block tensor by optimal reweighting of the singular vectors of the measurement matrix. Finally, the recovered 3-D seismic data are obtained by applying the inverse CWT on the transformed dimensions of seismic data. The proposed methodology is described as

## III. EXAMPLES AND RESULTS

Two synthetic data and a field 3-D seismic data example were considered to investigate the capabilities and deficiencies of the proposed method. Results were compared with the competitive t-OSSVD, BM4D, and IBTSVT methods. The performance of the proposed method in suppressing random noise could be evaluated using different qualitative and quantitative analyzing tools. The average amplitude spectrum is the general qualitative evaluation tool in random noise suppression. This evaluation tool, however, requires predefinition of the noise-free signal. The other evaluation tool is the signal-to-noise ratio (SNR),  $SNR = 10 \log(\frac{P_{\text{signal}}}{P_{\text{noise}}})$ , where  $P_{\text{signal}}$  and  $P_{\text{noise}}$  are the power of the noise-free signal and the noise, respectively. Visual inspection of the residual section, which is the subtraction of the denoised signal from the original signal, could provide qualitative information about the performance of the noise removal method and possible distortion of the signal.

### A. Synthetic 3-D Seismic Data

The synthetic data examples that were selected for investigating the performance of the proposed method is illustrated in Fig. 1(a). The modeled 3-D data cube contains a flat horizontal event and a dipping event, both faulted by two vertical faults,

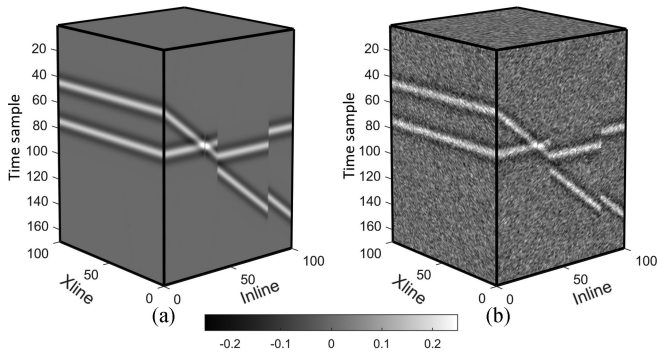


Fig. 1. (a) Synthetic seismic data with faulted horizontal and dipping events and (b) the data contaminated by random noise.

contaminated by random noise [see Fig. 1(b)]. The synthetic seismic data contain 10 000 seismic traces distributed horizontally with 170 time samples in the vertical direction. To simulate the seismic signal, the source wavelet was a Ricker wavelet with 35 Hz dominant frequency and 2 ms sampling interval. The seismic data shown in Fig. 1(b) are contaminated by  $-4$  dB white Gaussian noise. To fully consider the capabilities of the proposed method, results were also compared by the t-OSSVD, BM4D, and IBTSVT methods. In this article, the essential parameters for comparison methods were selected so that to have the best performance for each method. Since the synthetic data contains two seismic events, thus the rank parameter for low-rank component extraction was selected as 2. The Morlet wavelet was selected for low-rank extraction, and the tensor size was defined as  $100 \times 100 \times 340$ . In the t-OSSVD method, the value for the parameter aspect ratio was selected as 1. It was shown in [22] that the t-OSSVD method exhibits the best performance in random noise elimination when this parameter is selected as 1. The tensor size for the t-OSSVD method was selected as  $100 \times 100 \times 340$ . The standard deviation in the t-OSSVD and the proposed algorithms would be defined based on the characteristics of seismic data. In the IBTSVT algorithm, the seismic data will be initially divided into smaller blocks and the algorithm would be applied separately on each block. The size of each block was considered as  $5 \times 5 \times 680$ . The thresholding parameter in this data for the IBTSVT algorithm was defined by  $\tau = 680 / \sqrt{n_1 n_2}$ . The process of denoising is affected by modifying two parameters, namely block size and thresholding parameter in this method. The block size should not be very high, as this causes the low-rank component to interact with the sparse section. The computational cost will be raised if the block size is set too small due to the large number of t-SVDs. It is difficult to figure out the thresholding parameter  $\tau$ . It can be chosen based on personal experience. The parameters in the BM4D method were considered the same as in the t-OSSVD algorithm. The only difference for the BM4D method is the random noise's nature, which was considered the Gaussian noise. The number of iterations for all methods, except for the BM4D, was considered as 14. Fig. 2(a)–Fig. 2(d) shows the noise attenuation results of the proposed method, t-OSSVD, IBTSVT, and BM4D, respectively. The IBTSVT algorithm could not perform noise suppression as well as other competitive methods. Visual inspection on the t-OSSVD and the proposed method shows that both these methods are comparable and better than the BM4D method. For better comparison of capabilities of these methods, the residual cube, as the result of

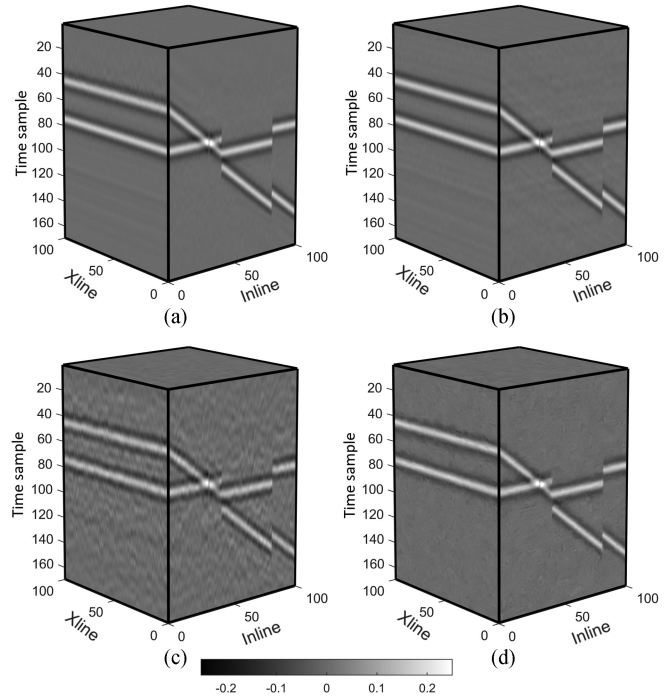


Fig. 2. Noise attenuation from seismic data shown in Fig. 1 by the (a) proposed method, (b) t-OSSVD, (c) IBTSVT, and (d) BM4D methods.

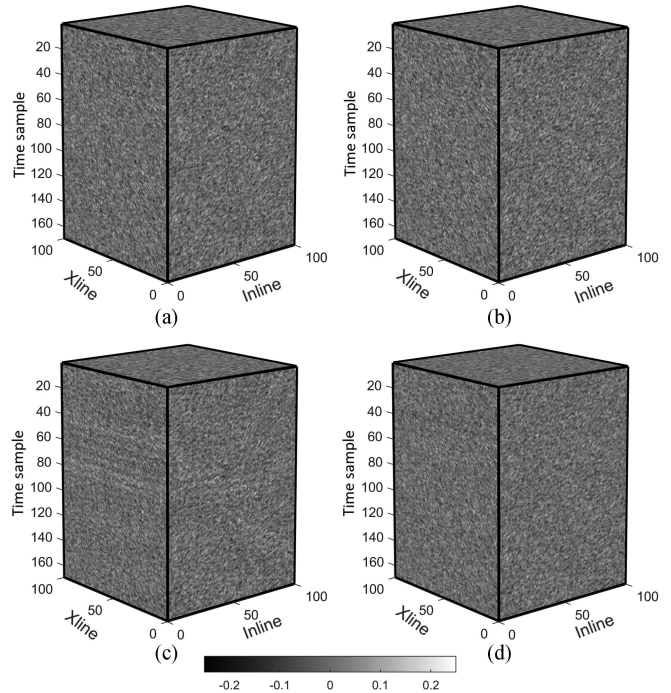


Fig. 3. The residual cube or the noise attenuated from seismic data shown in Fig. 1 by the (a) proposed method, (b) t-OSSVD, (c) IBTSVT, and (d) BM4D methods.

subtracting the noise suppressed cube from the original noisy data, is illustrated in Fig. 3. As it could be seen, some of the remaining seismic events are present in the residual cubes of the IBTSVT and BM4D, which indicates the poor performance of these two methods compared to the t-OSSVD and proposed algorithms. Apparently, more random noise has been eliminated

TABLE I  
SNR OF THE DENOISED DATA FROM THE SELECTED NOISE SUPPRESSION METHODS ON THE SYNTHETIC DATA SHOWN IN FIG. 1

Noise suppression method	proposed	t-OSSVD	BM4D	IBTSVT
The SNR value	19.3	18.1	12.7	7.6

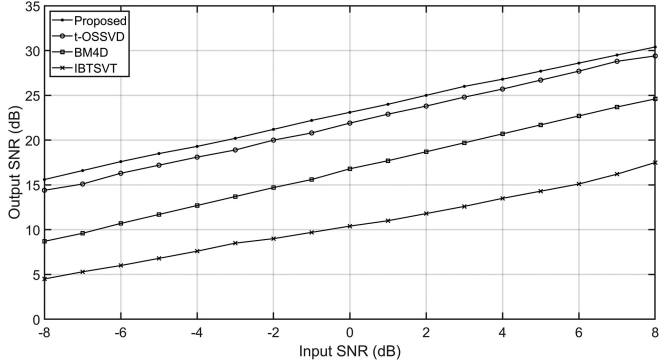


Fig. 4. Investigation on robustness and performance of the proposed and other competitive random noise suppression methods against different input SNR values for the first synthetic data example. They all show linear behavior and the proposed method give higher output SNR for all input SNR values.

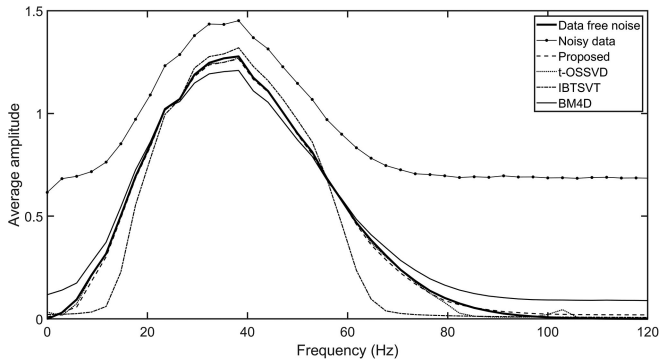


Fig. 5. Average amplitude spectrum of noise-free data, noisy data, and denoised data obtained by the proposed method and other selected competitive noise suppression methods for the first synthetic data example. The proposed method and the t-OSSVD both give closer spectrum to that of noise-free data rather than other noise attenuation algorithms.

by the proposed algorithm and the t-OSSVD method. However, no distinct difference between the results of these two methods could be defined by visual inspection. The SNR could provide a better quantitative comparison between all these noise suppression algorithms. The result of this comparison is presented in Table I. While IBTSVT and BM4D exhibit low SNR, the proposed method gives higher SNR compared to t-OSSVD. Besides evaluating the amount of random noise eliminated by each method, each noise suppression method's performance and robustness should also be tested against diverse SNR for the input data. Fig. 4 shows the results of this experiment. All methods exhibit linear behavior for different input SNR values and predict output SNR. This evaluation reveals that the proposed method gives a higher SNR for all various input values. The performance of these methods could be investigated more by comparing the average amplitude spectrum for denoised seismic data provided by each method with the average amplitude spectrum of the original noise-free data. Fig. 5 shows the results. The IBTSVT

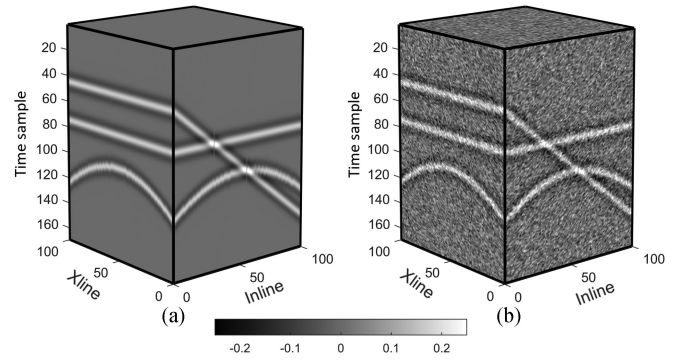


Fig. 6. (a) Noise free synthetic data of the second data example and (b) same data contaminated by  $-4$  dB random noise.

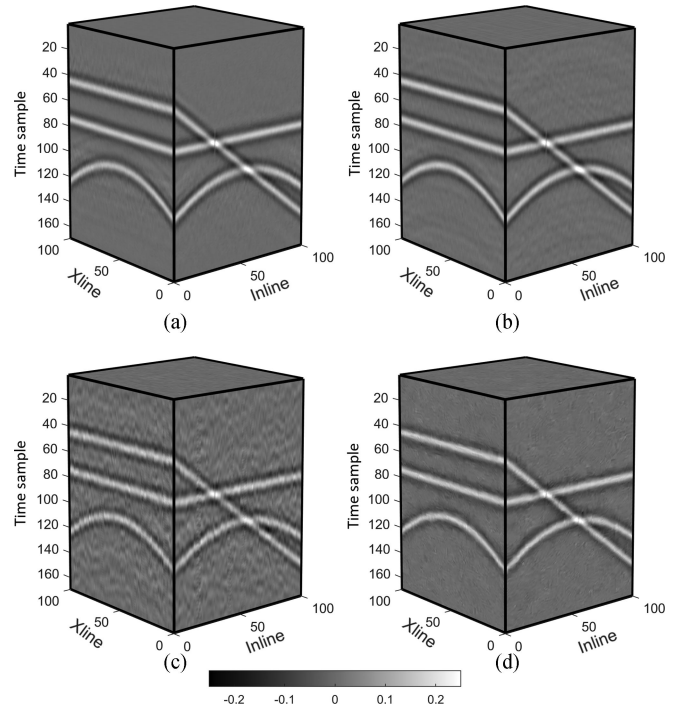


Fig. 7. Noise attenuation from seismic data shown in Fig. 6 by the (a) proposed method, (b) t-OSSVD, (c) IBTSVT, and (d) BM4D methods.

method could not recover the original amplitude of the seismic signals, while the BM4D shows a higher amplitude for seismic data at the two ends of the spectrum. Again, here the proposed method and the t-OSSVD exhibit comparable performance. Therefore, it can be concluded that the proposed method has acceptable performance in noise suppression of seismic data. A more complex model was used to simulate synthetic seismic data to better evaluate the method's capabilities. Fig. 6(a) shows the data, which contains horizontal, dipping, and dome shape seismic events. Fig. 6(a) shows noise-free data and Fig. 6(b) shows the data contaminated by  $-4$  dB random noise. The parameters of the noise suppression methods are the same as those used in the previous example. However, since the second synthetic data example contains three seismic events, the low-rank parameter order should be considered 3. The thresholding parameter was defined by  $\tau = \frac{800}{\sqrt{n_1 n_2}}$ . Fig. 7(a)–Fig. 7(d) shows noise attenuation results. The IBTSVT and the BM4D could not provide high-quality results like the proposed method

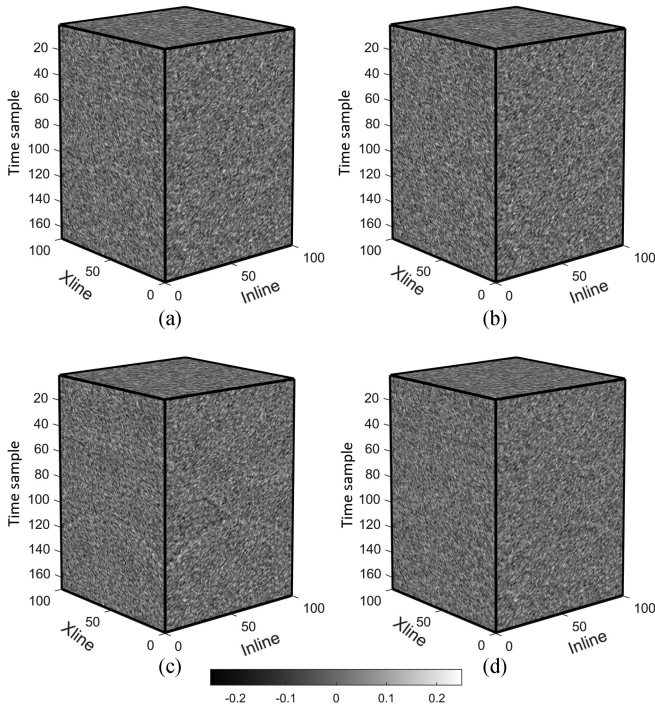


Fig. 8. Residual cube of the noise attenuated from seismic data shown in Fig. 6 by the (a) proposed method, (b) t-OSSVD, (c) IBTSVT, and (d) BM4D methods.

TABLE II  
SNR OF THE DENOISED DATA FROM THE SELECTED NOISE SUPPRESSION METHODS ON THE SYNTHETIC DATA SHOWN IN FIG. 6

Noise suppression method	proposed	t-OSSVD	BM4D	IBTSVT
The SNR value	15.1	13.9	11.9	6.6

and conventional t-OSSVD methods. More random noise is still present in Fig. 7(c), which is the result of IBTSVT. The result of the BM4D method also is not comparable with denoised seismic cubes with the t-OSSVD and proposed method. Visual inspection of results with the t-OSSVD and the proposed method reveals that noise suppression provides more clear data. Fig. 8 illustrates the residual cube for each method after the denoising procedure. While the IBTSVT removed some reflection signals, the BM4D could not clear noisy data as much as the proposed method and the t-OSSVD approach. Table II shows a quantitative comparison of results with the SNR values. The proposed method has provided higher SNR than all competitive methods, which depicts its capability and better performance in suppressing random noise. Performance of the selected denoising methods for the second synthetic data example, which is more geometrically complicated, against various input SNR is shown in Fig. 9. The IBTSVT method still exhibits poor performance in all input SNR, but the BM4D method behaves differently in dealing with low-input SNR and high-input SNR values. The BM4D method gives the highest SNR for large input SNR values, while for most of the input SNR values in the selected range, the proposed approach still gives higher SNR. The average amplitude spectrum of noise-free data and noisy data are illustrated with the average amplitude spectrum of denoised data in Fig. 10. The BM4D method does not exhibit a similar curve for the average amplitude as the noise-free data for

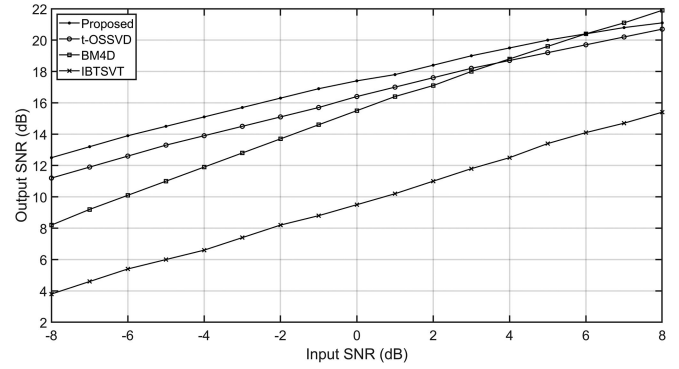


Fig. 9. Investigation on the robustness and the performance of the proposed and other competitive random noise suppression methods against different input SNR values for the second synthetic data example shown in Fig. 6. They all show somehow linear behavior and the proposed method gives higher output SNR for all input SNR values.

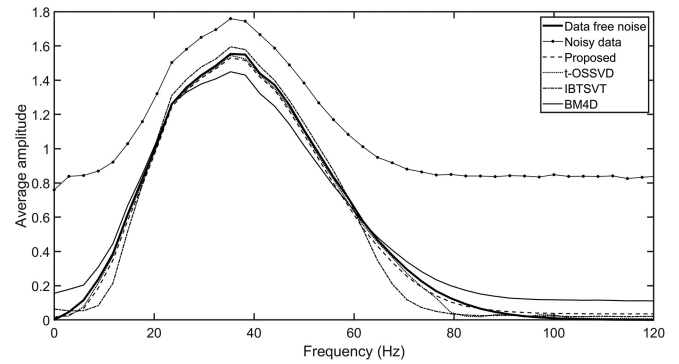


Fig. 10. Average amplitude spectrum of noise-free data, noisy data, denoised data by the proposed method and denoised data by other selected competitive noise suppression methods for the second synthetic data example. The proposed method and the t-OSSVD both give closer spectrum to noise-free data rather than other noise attenuation algorithms.

most of the frequencies in the spectrum. The IBTSVT method also fails to provide average amplitudes as the noise-free data accurately. The proposed approach and the t-OSSVD method exhibit similar curves for the average amplitude as the noise-free seismic data. Although applying the proposed approach on two synthetic data examples confirms its reliable performance on suppressing random noise in seismic data, it needs to be applied on seismic field data and its performance should be evaluated in handling random noise attenuation.

### B. Application on Field Data Example

The selected field data for this study is a portion of a large 3-D marine seismic data with  $231 \times 311$  seismic traces distributed in in-line–X-line plane. The sampling rate is 4 ms and 100 time samples were selected in the vertical time direction (see Fig. 11). The data contain both horizontal and dipping reflectors folded and faulted due to the upward movement of a salt dome. However, the salt dome itself is not shown in the selected portion of the cube. The data do not have a high quality and suffers from a considerable level of random noise. From the geometrical point of view, it could also be considered semicomplicated data. The proposed approach was applied to data and the three other selected competitive methods. The best performance of the proposed method was obtained with the rank value of 70 and

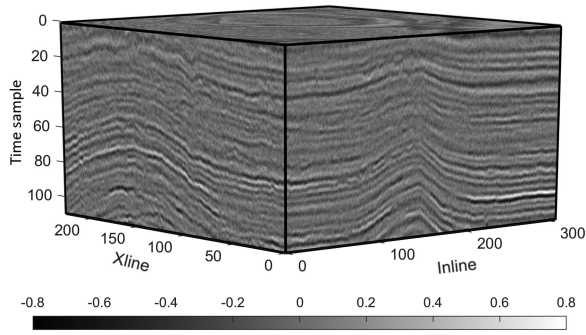


Fig. 11. Field 3-D seismic data from marine data acquisition.

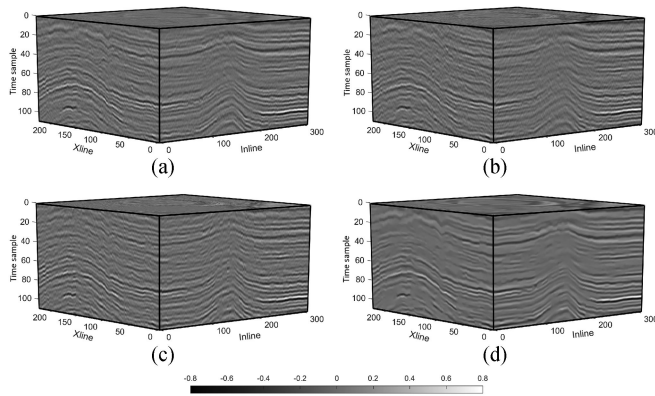


Fig. 12. Residual cube or the noise attenuated from seismic data shown in Fig. 1 by the (a) proposed method, (b) t-OSSVD, (c) IBTSVT, and (d) BM4D methods.

the Morlet wavelet for CWT analysis. The size of the selected tensor for the proposed method was  $231 \times 311 \times 220$ . In the t-OSSVD algorithm, the aspect ratio parameter was selected as 1, the balancing sparsity parameter considered as 0.1, and the size of the tensor was  $231 \times 311 \times 220$ . The best performance for the IBTSVT method was obtained with the thresholding parameter defined by  $\tau = \frac{210}{\sqrt{n_1 \times n_2}}$  and the block size was considered as  $5 \times 5 \times 660$ . For the BM4D method, all the parameters were selected the same as its previous application on synthetic data examples. Fig. 12 shows a denoised seismic cube after applying these methods. Initial inspection of the results shows a dramatic change in data quality after applying the denoising procedure. However, more visual inspection reveals that in some cases, as in the BM4D result, this quality increases in data costs to lose some parts of signal and deterioration in reflectors. The t-OSSVD method removed some small amounts of the signal and could not remove parasites from the seismic data, which are obvious in all horizontal reflectors. The IBTSVT method has preserved the seismic signal more than the BM4D and the t-OSSVD methods, but it could not remove a sufficient amount of random noise and does not provide higher quality in data compared to other methods. Nevertheless, the proposed method preserved the signals while removing sufficient random noise. The result of the proposed method may suffer from parasites. However, they did not deteriorate the geometry of the reflectors in data. Fig. 13 shows the residual cube of the field data example for all denoising methods applied on the original noisy data. As it could be seen in Fig. 13, the BM4D and the t-OSSVD methods have removed some parts of the signal, which are present in the

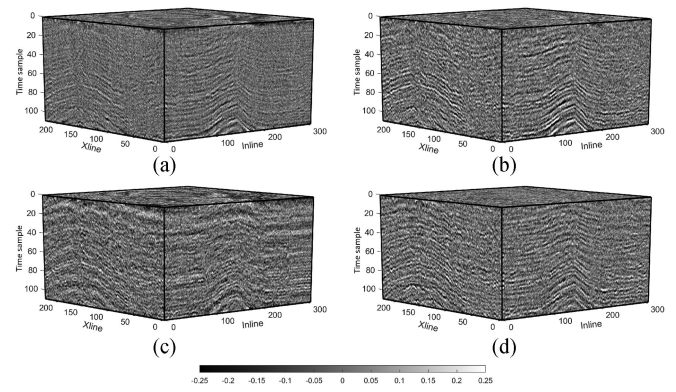


Fig. 13. Residual cube, which is the result of subtracting denoised data from the original noisy data for the field seismic data example. Residual cubes of (a) the proposed method, (b) the t-OSSVD noise suppression method, (c) the IBTSVT noise removal method, and (d) the BM4D noise attenuation method.

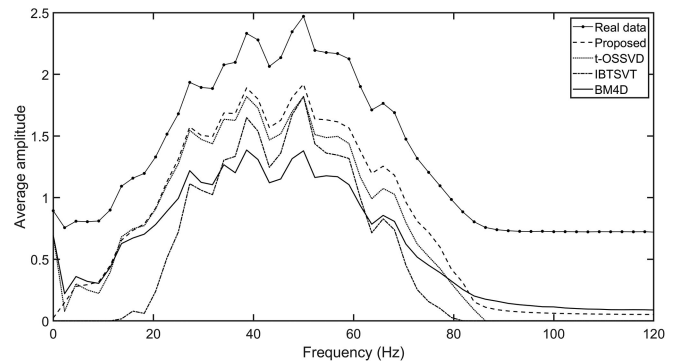


Fig. 14. Average amplitude spectrum of noise-free data, noisy data, and denoised data by the proposed method and denoised data by other selected competitive noise suppression methods for the field seismic data example.

residual cubes. The IBTSVT method has not removed sufficient noise compared to the proposed method. The residual cube of the proposed method exhibits more suppressed random noise compared to other residual cubes by other methods, which depicts its better performance in the denoising procedure. A comparison of the average amplitude spectrum of denoised data by four methods with that of the original seismic data is shown in Fig. 14. The BM4D and the IBTSVT methods could not provide an average amplitude spectrum close to the original seismic data as the t-OSSVD and the proposed methods. Nevertheless, the average amplitude curves of the t-OSSVD and the proposed methods coincide for some frequency ranges, but in most frequency bands, the proposed method provides a better result, except in higher frequency values, which is not in the range for the desired signal. Since no noise-free data are available for the field data example, thus results could not be compared by means of the SNR criterion. We chose a 2-D section in the in-line direction of number 5 to investigate the robustness of the selected approaches with respect to variations in the shape of seismic signals, which is illustrated in Fig. 15. Results of denoising methods are also provided in Fig. 16 for this specific area to showcase performance of denoising methods. As can be observed, the T-OSSVD approach leaves a significant amount of random noise in the data. The amplitudes of the reflectors are likewise suppressed by the BM4D and IBTSVT approaches, and it appears that the signal is partially erased by this method.

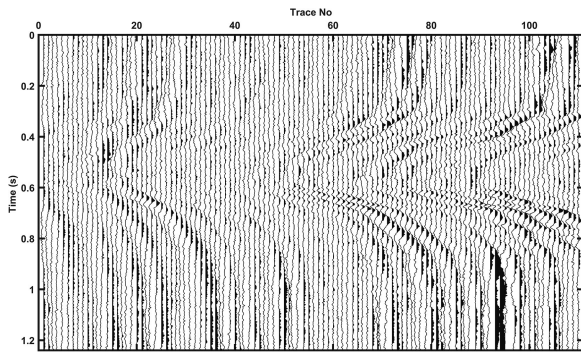


Fig. 15. Vertical slice derived from real 3-D seismic data along the in-line direction number 5 from Fig. 11.

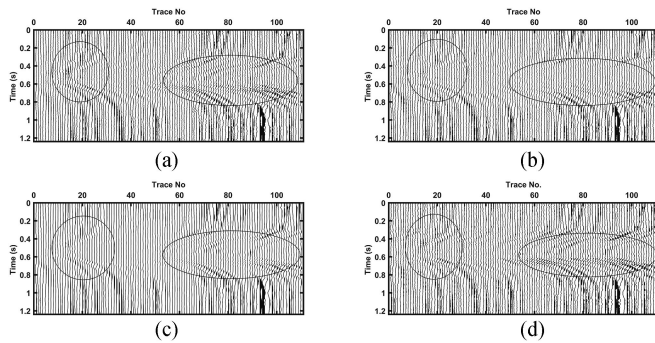


Fig. 16. Denoising of a vertical section using (a) the proposed, (b) the T-OSSVD, (c) the BM4D, and (d) the IBSTVT methods on 3-D real seismic data (see Fig. 11) along in-line direction number 5.

As a result, the proposed technique can better attenuate random noise while preserving the data signal.

#### IV. CONCLUSION

Application of the proposed method introduced here depicted that this method could efficiently suppress random noise while keeping the data's signal content more effectively compared to the other competitive methods. The algorithm of the proposed method is straightforward in application and benefits from automatic optimization in coefficients and parameters, which will dramatically reduce the computation time. The proposed method is not complicated in implementation and application and thus could be applied easily on 3-D seismic data. The SNR in denoised data obtained by the proposed method in two synthetic data examples was higher than other methods. Besides comparing residual data and average amplitude spectrum, the visual inspection revealed a more effective noise elimination of the proposed method. Investigation on residual data in the real field seismic data example depicted that the proposed method will not deteriorate the shape of the seismic signal. In contrast, other methods, somehow, have changed the shape of the seismic signal, and thus will result in false geological interpretation. The BM4D and the IBSTVT methods changed the shape of seismic events and thus will not provide reliable denoised data. The t-OSSVD method, although it does not suffer from this problem, but will not preserve signals as much as the proposed method. So, the proposed method could be known as a cost and time-effective random noise attenuation algorithm, specifically

for large 3-D seismic data, contaminated by high level of random noise and acquired from complex subsurface media.

#### REFERENCES

- [1] G. Li, Y. Li, and B. Yang, "Seismic exploration random noise on land: Modeling and application to noise suppression," *IEEE Trans. Geosci. Remote Sens.*, vol. 55, no. 8, pp. 4668–4681, Aug. 2017.
- [2] R. Anvari, A. R. Kahoo, M. Mohammadi, N. A. Khan, and Y. Chen, "Seismic random noise attenuation using sparse low-rank estimation of the signal in the time-frequency domain," *IEEE J. Sel. Topics Appl. Earth Observ. Remote Sens.*, vol. 12, no. 5, pp. 1612–1618, May 2019.
- [3] Y. Chen, X. Chen, Y. Wang, and S. Zu, "The interpolation of sparse geophysical data," *Surv. Geophys.*, vol. 40, no. 1, pp. 73–105, 2019.
- [4] B. Liu, C. Fu, Y. Ren, Q. Zhang, X. Xu, and Y. Chen, "Structural complexity-guided predictive filtering," *Geophys. Prospecting*, vol. 68, no. 5, pp. 1509–1522, 2020.
- [5] Z. Geng, X. Wu, S. Fomel, and Y. Chen, "Relative time seislet transform," *Geophysics*, vol. 85, no. 2, pp. V223–V232, 2020.
- [6] N. Kreimer and M. D. Sacchi, "A tensor higher-order singular value decomposition for prestack seismic data noise reduction and interpolation," *Geophysics*, vol. 77, no. 3, pp. V113–V122, 2012.
- [7] W. Gao and M. D. Sacchi, "Random noise attenuation via the randomized canonical polyadic decomposition," *Geophys. Prospecting*, vol. 68, no. 3, pp. 872–891, 2020.
- [8] M. Naghizadeh and M. Sacchi, "Multidimensional de-aliased Cadzow reconstruction of seismic records," *Geophysics*, vol. 78, no. 1, pp. A1–A5, 2013.
- [9] R. Anvari, M. Mohammadi, A. R. Kahoo, N. A. Khan, and A. I. Abdullah, "Random noise attenuation of 2D seismic data based on sparse low-rank estimation of the seismic signal," *Comput. Geosci.*, vol. 135, Art. no. 104376, 2020.
- [10] S. Amani, A. Gholami, and A. J. Niestanak, "Seismic random noise attenuation via 3d block matching," *J. Appl. Geophys.*, vol. 136, pp. 353–363, 2017.
- [11] A. Roueff, P. Roux, and P. Réfrégier, "Wave separation in ambient seismic noise using intrinsic coherence and polarization filtering," *Signal Process.*, vol. 89, no. 4, pp. 410–421, 2009.
- [12] Y. Chen, S. Fomel, and J. Hu, "Iterative deblending of simultaneous-source seismic data using seislet-domain shaping regularization," *Geophysics*, vol. 79, no. 5, pp. V179–V189, 2014.
- [13] J. Cheng, M. Sacchi, and J. Gao, "Computational efficient multidimensional singular spectrum analysis for prestack seismic data reconstruction," *Geophysics*, vol. 84, no. 2, pp. V111–V119, 2019.
- [14] V. Oropeza and M. Sacchi, "Simultaneous seismic data denoising and reconstruction via multichannel singular spectrum analysis," *Geophysics*, vol. 76, no. 3, pp. V25–V32, 2011.
- [15] J. Zhang, Y. Li, and N. Wu, "Noise attenuation for seismic data by hyperbolic-trace time-frequency peak filtering," *IEEE Geosci. Remote Sens. Lett.*, vol. 12, no. 3, pp. 601–605, Mar. 2015.
- [16] H. Lin, Y. Li, B. Yang, H. Ma, and C. Zhang, "Seismic random noise elimination by adaptive time-frequency peak filtering," *IEEE Geosci. Remote Sens. Lett.*, vol. 11, no. 1, pp. 337–341, Jan. 2014.
- [17] W.-L. Hou, R.-S. Jia, H.-M. Sun, X.-L. Zhang, M.-D. Deng, and Y. Tian, "Random noise reduction in seismic data by using bidimensional empirical mode decomposition and shearlet transform," *IEEE Access*, vol. 7, pp. 71374–71386, 2019.
- [18] Y. Liu, Y. Li, H. Lin, and H. Ma, "An amplitude-preserved time-frequency peak filtering based on empirical mode decomposition for seismic random noise reduction," *IEEE Geosci. Remote Sens. Lett.*, vol. 11, no. 5, pp. 896–900, May 2014.
- [19] X. Han, H. Lin, Y. Li, H. Ma, and X. Zhao, "Adaptive fission particle filter for seismic random noise attenuation," *IEEE Geosci. Remote Sens. Lett.*, vol. 12, no. 9, pp. 1918–1922, Sep. 2015.
- [20] Y. Chen, J. Ma, and S. Fomel, "Double-sparsity dictionary for seismic noise attenuation," *Geophysics*, vol. 81, no. 2, pp. V103–V116, 2016.
- [21] Y. Chen, "Fast dictionary learning for noise attenuation of multidimensional seismic data," *Geophys. J. Int.*, vol. 209, no. 1, pp. 21–31, 2017.
- [22] R. Anvari, M. Mohammadi, and A. R. Kahoo, "Enhancing 3D seismic data using the t-SVD and optimal shrinkage of singular value," *IEEE J. Sel. Topics Appl. Earth Observ. Remote Sens.*, vol. 12, no. 1, pp. 382–388, Jan. 2019.

- [23] Y. Chen, Y. Zhou, W. Chen, S. Zu, W. Huang, and D. Zhang, "Empirical low-rank approximation for seismic noise attenuation," *IEEE Trans. Geosci. Remote Sens.*, vol. 55, no. 8, pp. 4696–4711, 2017.
- [24] R. Anvari, M. A. N. Siahshar, S. Gholtashi, A. R. Kahoo, and M. Mohammadi, "Seismic random noise attenuation using synchrosqueezed wavelet transform and low-rank signal matrix approximation," *IEEE Trans. Geosci. Remote Sens.*, vol. 55, no. 11, pp. 6574–6581, Aug. 2017.
- [25] T. Zhou and D. Tao, "GoDec: Randomized low-rank & sparse matrix decomposition in noisy case," in *Proc. 28th Int. Conf. Mach. Learn.*, 2011, pp. 33–40.
- [26] Y. Chen and S. Fomel, "EMD-seislet transform," *Geophysics*, vol. 83, no. 1, pp. A27–A32, 2018.
- [27] D. Bonar and M. Sacchi, "Denoising seismic data using the nonlocal means algorithm," *Geophysics*, vol. 77, no. 1, pp. A5–A8, 2012.
- [28] R. Vautard, P. Yiu, and M. Ghil, "Singular-spectrum analysis: A toolkit for short, noisy chaotic signals," *Physica D: Nonlinear Phenomena*, vol. 58, nos. 1/4, pp. 95–126, 1992.
- [29] M. A. Nazari Siahshar, S. Gholtashi, A. R. Kahoo, H. Marvi, and A. Ahmadifard, "Sparse time-frequency representation for seismic noise reduction using low-rank and sparse decomposition," *Geophysics*, vol. 81, no. 2, pp. V117–V124, 2016.
- [30] S. K. Chiu, "Coherent and random noise attenuation via multichannel singular spectrum analysis in the randomized domain," *Geophys. Prospecting*, vol. 61, pp. 1–9, 2013.
- [31] E. J. Candes and Y. Plan, "Matrix completion with noise," *Proc. IEEE Proc. IRE*, vol. 98, no. 6, pp. 925–936, Jun. 2010.
- [32] Y. Peng, A. Ganesh, J. Wright, W. Xu, and Y. Ma, "RASL: Robust alignment by sparse and low-rank decomposition for linearly correlated images," *IEEE Trans. Pattern Anal. Mach. Intell.*, vol. 34, no. 11, pp. 2233–2246, Nov. 2012.
- [33] R. Anvari, A. R. Kahoo, M. Mohammadi, and A. A. Pouyan, "Random noise attenuation in 3D seismic data by iterative block tensor singular value thresholding," in *Proc. 3rd Iranian Conf. Intell. Syst. Signal Process.*, 2017, pp. 164–168.
- [34] A.-H. Najmi *et al.*, "The continuous wavelet transform and variable resolution time-frequency analysis," *Johns Hopkins APL Tech. Dig.*, vol. 18, no. 1, pp. 134–140, 1997.
- [35] R. Cabieces *et al.*, "Slowness vector estimation over large-aperture sparse arrays with the continuous wavelet transform (CWT): Application to ocean bottom seismometers," *Geophys. J. Int.*, vol. 223, no. 3, pp. 1919–1934, 2020.
- [36] Y. Wang, "Frequencies of the Ricker wavelet," *Geophysics*, vol. 80, no. 2, pp. A31–A37, 2015.
- [37] L. Chen, Y. Liu, and C. Zhu, "Iterative block tensor singular value thresholding for extraction of lowrank component of image data," in *Proc. IEEE Int. Conf. Acoust. Speech Signal Process.*, 2017, pp. 1862–1866.
- [38] M. Gavish and D. L. Donoho, "Optimal shrinkage of singular values," *IEEE Trans. Inf. Theory*, vol. 63, no. 4, pp. 2137–2152, Apr. 2017.
- [39] R. R. Nadakuditi, "OptShrink: An algorithm for improved low-rank signal matrix denoising by optimal, data-driven singular value shrinkage," *IEEE Trans. Inf. Theory*, vol. 60, no. 5, pp. 3002–3018, May 2014.



**Javad Mafakheri** received the B.S. degree in physics from Bu Ali Sina University, Hamadan, Iran, in 2016, and the M.S. degree in exploration seismology from the Shahrood University of Technology, Shahrood, Iran, in 2020.

His research interests include the application of time-frequency analysis and denoising of seismic data in seismic data processing.



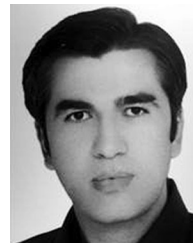
**Amin Roshandel Kahoo** received the B.S. degree in mineral exploration from Birjand University, South Khorasan, Iran, in 2002, and the M.S. and Ph.D. degrees in exploration seismology from Tehran University, Tehran, Iran, in 2005 and 2010, respectively.

He is currently an Associate Professor with the Shahrood University of Technology, Shahrood, Iran. His research interests include the application of sparse time-frequency analysis and compressed sensing theory in seismic data processing and interpretation.



**Rasoul Anvari** received the Bachelor of Science degree in physics from Razi University, Kermanshah, Iran, in 2015, and the Master of Science degree in exploration seismology from the Shahrood University of Technology, Shahrood, Iran in 2017.

His research interests include the application of time-frequency analysis, machine learning, deep learning, denoising, and reconstruction of seismic data in seismic data processing and interpretation.



**Mokhtar Mohammadi** received the B.S. degree in computer engineering from Shahed University, Tehran, Iran, in 2003, the M.S. degree in Computer Engineering from Shahid Beheshti University, Tehran, Iran, in 2012, and the Ph.D. degree in computer engineering from Shahrood University of Technology, Shahrood, Iran, in 2018.

He is currently with the Department of Information Technology, College of Engineering and Computer Science, Lebanese French University, Kurdistan, Iraq. His current research interests include signal

processing, time-frequency analysis, and machine learning.



**Mohammad Radad** received the bachelor's degree in applied physics from the Shahrood University of Technology, Shahrood, Iran, in 2005, and the M.Sc. and Ph.D. degrees in geophysics (exploration seismology) from the University of Tehran, Tehran, Iran, in 2009 and 2015, respectively.

He is currently an Assistant Professor of geophysics with the Shahrood University of Technology. His research interests include time-frequency analysis, seismic signal processing and seismic attributes.



**Mehrdad Soleimani Monfared** received Bachelor and Master of Science in mining exploration and Ph.D. in exploration seismology from the Shahrood University of Technology, Iran, where he is an academic staff in the seismology group. His research interest is seismic imaging and seismic data analysis. Now he is a visiting scientist in the Geophysical Institute (GPI) Institute, Karlsruhe Institute of Technology (KIT), Germany, working on the full waveform Inversion(FWI) method.